



MIT Open Access Articles

Parasitic capacitance cancellation in filter inductors

The MIT Faculty has made this article openly available. **Please share** how this access benefits you. Your story matters.

Citation	Neugebauer, T. C., and D. J. Perreault. "Parasitic Capacitance Cancellation in Filter Inductors." IEEE Trans. Power Electron. 21, no. 1 (Jan. 2006): 282–288.
As Published	http://dx.doi.org/10.1109/TPEL.2005.861103
Publisher	Institute of Electrical and Electronics Engineers (IEEE)
Version	Final published version
Citable link	http://hdl.handle.net/1721.1/86913
Terms of Use	Article is made available in accordance with the publisher's policy and may be subject to US copyright law. Please refer to the publisher's site for terms of use.

Parasitic Capacitance Cancellation in Filter Inductors

Timothy C. Neugebauer and David J. Perreault, *Member, IEEE*

Abstract—This paper introduces a technique for improving the high-frequency performance of filter inductors and common-mode chokes by cancelling out the effects of parasitic capacitance. This technique uses additional passive components to inject a compensation current that cancels the parasitic current, thereby improving high-frequency filtering performance. Two implementation approaches for this technique are introduced. The first implementation achieves cancellation using an additional small winding on the filter inductor and a small capacitor. This approach is effective where very high coupling of the windings can be achieved or where only moderate performance improvements are required. The second implementation utilizes a small radio frequency transformer in parallel with the filter inductor to inject cancellation currents from the compensation capacitor. This technique requires an additional component (the transformer), but can provide a high degree of cancellation. Experimental results confirm the theory in both implementations.

Index Terms—Common-mode chokes, filter inductors, RF (radio frequency) transformer.

I. INTRODUCTION

FILTER inductors and common-mode chokes suffer from both parasitic resistance and capacitance. Winding resistance and core loss lead to parasitic resistance, while parasitic capacitance arises from capacitance between winding turns and from winding-to-core capacitance. The distributed parasitic components can be lumped together to form the lumped-parameter model for an inductor shown in Fig. 1(a) [1]–[4]. The impedance magnitude of a practical inductor as a function of frequency is illustrated in Fig. 1(b). The parasitic capacitance dominates the impedance above the self-resonant frequency of the inductor (typically 1–10 MHz for power electronics applications, but sometimes lower for ungapped common-mode chokes). This parasitic capacitance reduces the impedance of an inductor at high frequencies, and hence reduces its effectiveness for high frequency filtering.

This paper introduces a technique for improving the high-frequency performance of filter inductors by cancelling out the effects of the parasitic capacitance. This technique uses additional passive components to inject a compensation current that cancels the current flowing through the parasitic capacitance, thereby improving high-frequency filtering performance. The proposed technique is related to strategies that have been exploited for reducing common-mode noise in certain power

Manuscript received August 30, 2004; revised April 6, 2005. This work was presented in part at the Power Electronics Specialist Conference, Aachen, Germany, 2005. This work was supported by the U.S. Office of Naval Research under ONR Grants N00014-00-1-0381 and N00014-02-1-0481. Recommended by Associate Editor T. Lebey.

T. C. Neugebauer is with Draper Laboratories, Cambridge, MA 02139-3563 USA (e-mail: neugebat@alum.mit.edu).

D. J. Perreault is with the Massachusetts Institute of Technology, Cambridge, MA 02139 USA (e-mail: djperrea@mit.edu).

Digital Object Identifier 10.1109/TPEL.2005.861103

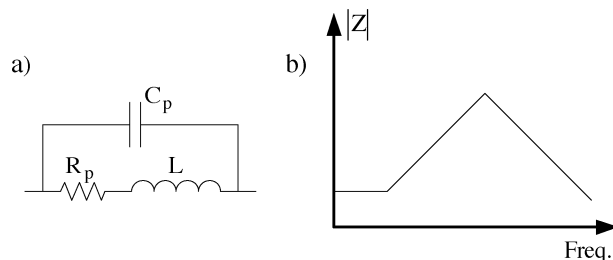


Fig. 1. Simple inductor model including parasitic effects. An impedance versus frequency plot shows that the capacitance limits the impedance at high frequencies.

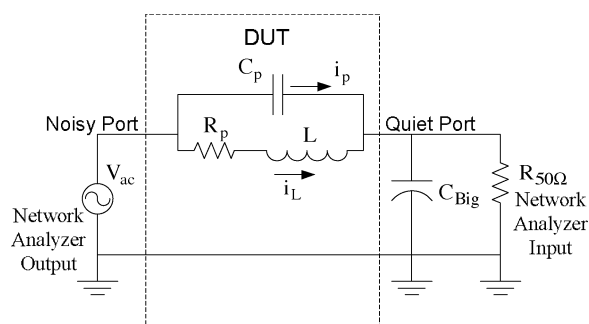


Fig. 2. Test circuit for evaluating the filtering performance of magnetic components. The device under test (DUT) is a filter inductor.

supply topologies [5]–[10], and is applicable to a wide range of filtering and power conversion designs where the parasitic feedthrough of magnetic components is an important consideration.

II. CAPACITANCE CANCELLATION

The proposed technique improves the performance of magnetic components (e.g., inductors and common-mode chokes) in filter applications where the function of the component is to prevent the transmission of high-frequency current from a “noisy” port to a “quiet” port. We assume that the “quiet” port is shunted by a sufficiently low impedance (e.g., a capacitor) that it is effectively at ac ground, and that small amounts of high-frequency current into the “noisy” port are acceptable so long as they are not transmitted to the “quiet” port. These assumptions are satisfied in a wide range of filtering and power conversion applications. A test circuit for evaluating the attenuation performance of filters is illustrated in Fig. 2. The “noisy” port of the device under test is driven from the output of a network analyzer, and the response at the “quiet” port is measured at the 50- Ω input of the network analyzer.

The capacitance cancellation technique developed here is not geared toward changing the parasitic capacitance itself (i.e., the capacitance C_p of the device under test in Fig. 2). Rather, the deleterious effect of the parasitic capacitance—the current that

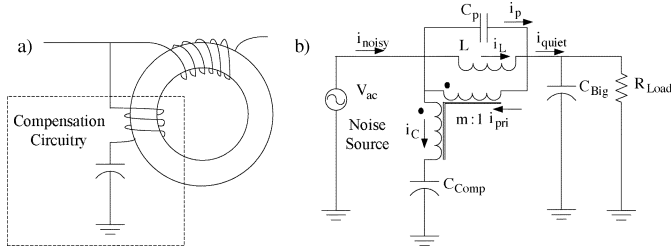


Fig. 3. (a) Additional winding and a capacitor are added to the inductor to form the circuit for parasitic capacitance cancellation and (b) equivalent circuit of (a) in the test circuit of Fig. 2.

passes through it at high frequencies—is nullified by a counterbalancing current injected at the quiet port. This counterbalancing current is injected by passive circuitry introduced expressly for this purpose. Referring to Fig. 2 (where an inductor and its parasitics form the device under test), the quiet port is assumed to be at ac ground, so the voltage across the device under test is the ac component of the voltage at the noisy port. The capacitor current, i_p , injected into the quiet port by the noisy port voltage v_{ac} at the angular frequency ω can thus be expressed as

$$i_p = j\omega v_{ac} C_p. \quad (1)$$

The goal of cancelling the current i_p at the quiet port can be achieved by adding an additional compensation winding and capacitor to the inductor, as illustrated in Fig. 3(a). The compensation winding carries only small, high-frequency currents, and can be implemented with very small wire. As shown in Fig. 3(b), the compensation winding forms a transformer with the main winding, with the magnetizing inductance operating as the filter inductor. Neglecting other transformer parasitics (such as leakage) the circuit operation can be described as follows: The net current injected into the quiet port can be calculated as

$$i_{\text{quiet}} = \frac{v_{ac}}{j\omega L} + j\omega v_{ac} [C_p - m(1-m)C_{\text{Comp}}] \quad (2)$$

where m is the ratio of the compensating winding turns to the main winding turns, and C_{Comp} is the value of the compensation capacitor. By selecting the winding ratio and compensation capacitor such that $m(1-m)C_{\text{Comp}} = C_p$, the parasitic capacitance current injected into the quiet port is cancelled by the compensation circuit, leaving only the inductive current component.

While this technique eliminates the effect of the parasitic capacitance at the quiet port, it does not eliminate the parasitic effects in other regards. Most notably, the current into the noisy port actually increases at high frequencies. For any selection of winding ratio and compensation capacitor described above, the currents i_p and i_{pri} will ideally cancel out and the current from the noise source will be $i_L + I_C$ or

$$i_{\text{noisy}} = \frac{v_{ac}}{j\omega L} + j\omega v_{ac} C_p \frac{1}{m}. \quad (3)$$

Since m is selected to be < 1 to achieve cancellation at the quiet port, the capacitive current into the noisy port increases somewhat as compared to the uncanceled case. The additional current is the same as that of a small capacitor bypassing the noisy

port. In many applications this is quite acceptable, and it becomes advantageous in filter applications where a capacitive bypass of the noisy port is desirable.

The proposed compensation technique is related to a number of other filtering and balancing techniques that have been explored in the past. The topology of the filter network that is created [e.g., Fig. 3(b)] is identical to coupled inductor filter structures that have been used widely for everything from notch-filtering [11], [12] to “zero ripple” filters [13]–[17] to filters incorporating parasitic inductance cancellation [18], [19]. However, the design goals and component values of these other circuit implementations are vastly different from the case considered here. The technique presented here bears a closer relationship to recent work on cancellation of common-mode noise in certain switching-power supply topologies [5]–[10]. These use additional magnetics and capacitors to compensate common-mode currents injected from switching devices through the capacitance to the circuit ground or enclosure. The approach proposed here is different in that it focuses on parasitic capacitance appearing across magnetic components, and applies to a broad range of topologies and applications. Interestingly, these cancellation techniques are also related to the “neutralized” amplifier configurations developed more than fifty years ago, in which injected currents were used to compensate Miller capacitance effects in vacuum tube audio amplifiers [20], [21]. In this paper, we focus on the use of capacitance cancellation to enhance the performance of electrical filters. It is expected that the proposed approach will be less costly and burdensome to implement than more conventional electromagnetic interference (EMI) shielding techniques (e.g., a faraday shield) in many applications.

III. EVALUATION

To validate the proposed approach, a number of prototype circuits have been constructed and tested. For simplicity, the prototype circuits we describe here employ $m = 0.5$ and $C_{\text{Comp}} = 4C_p$ except as otherwise specified. This turns ratio can be easily achieved with a 1:1 center-tapped transformer by using the full winding of the primary and only half the winding on the secondary. The effects of varying the turns ratio will also be examined.

A prototype filter circuit with capacitance cancellation was constructed using one half of a P3219-A common-mode choke (Coilcraft, Inc., Cary, IL). Only one winding of the choke was used in the testing; the other winding was left unconnected. The main winding of this toroidal choke comprises 45 turns of 25-gauge wire in a single layer, forming a 10.8-mH filter inductance, with approximately 16 pF of parasitic capacitance. A compensation winding of 22 turns of AWG 30 wire was added to the choke, as illustrated in Fig. 3(a). A range of compensation capacitor values were tested to identify the best value and an 18-pF ceramic capacitor was selected. A 3.3-nF ceramic capacitor was used to bypass the quiet port.

The filter circuit was evaluated using the network analyzer-based test setup illustrated in Fig. 2. The filter circuit is driven from the network analyzer output, and the response at the quiet port is measured at the 50- Ω input of the network analyzer. Fig. 4 shows the magnitude of the transfer function from the noisy port to the quiet port over the conducted EMI frequency range (up

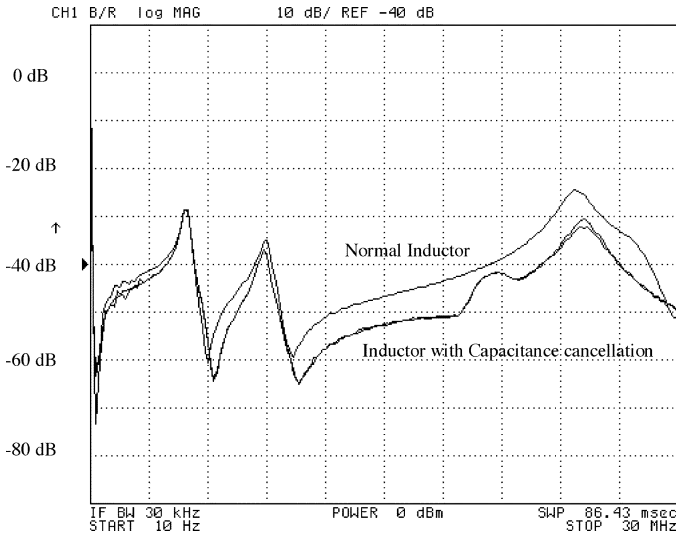


Fig. 4. Ratio of input to output voltage for the P3219-A Coilcraft choke. The higher curve is the response without the capacitance cancellation. Above 10 MHz there is about 7 dB of improvement from using the capacitance reduction technique. Note that the frequency scale is linear up to 30 MHz.

to 30 MHz) both with and without parasitic capacitance cancellation. As can be seen, the proposed cancellation technique improves performance by approximately 7 dB in the frequency range of 10 MHz to 28 MHz; tests on other devices provided similar results—a 5–10 dB improvement in performance at high frequencies. Most of the irregular peaks in the figure are due to higher frequency parasitics in the filter that are not modeled.

While the proposed cancellation technique does improve filter performance, the results are not as good as might be expected. The main source of this limitation is the leakage inductance of the cancellation transformer. All impedances in series with the compensation capacitor, especially the leakage inductance, will compromise the high frequency performance of the cancellation. Treating the leakage inductance of the compensation winding as part of a compensation impedance Z_{Comp} and ignoring the primary side leakage inductance, the quiet port current becomes

$$i_{quiet} = \frac{v_{ac}}{j\omega L} + j\omega v_{ac} C_p - \frac{m(1-m)}{Z_{Comp}(j\omega)} v_{ac} \quad (4)$$

$$i_{quiet} = \frac{v_{ac}}{j\omega L} + v_{ac} \frac{C_p C_{Comp} L_{Comp}(j\omega)^3}{C_{Comp} L_{Comp}(j\omega)^2 + 1} \quad (5)$$

where L_{Comp} is the secondary leakage inductance in series with C_{Comp} . The term $C_{Comp} L_{Comp}(j\omega)^2$ greatly affects the performance of capacitance cancellation. C_{Comp} is minimized when the turns ratio, m , is 1/2 and L_{Comp} is dependant on the magnetic element and is lower for transformers with a lower turns ratio. Thus, the coupling coefficient of the primary and cancellation windings is a critical factor in achieving good cancellation performance.

The transformer used in Fig. 4 was rewound such that the secondary has three turns resulting in a turns ratio of 0.06. The compensation capacitor was chosen to maximize the impedance of the inductor at frequencies lower than 6 MHz; the best compensation capacitors were experimentally determined to be 56 and 59 pF when the turns ratios are 0.5 and 0.06. Note that 56 pF is much larger than the expected compensating capacitor for

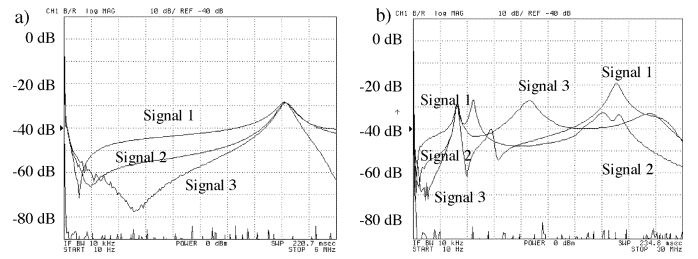


Fig. 5. Ratio of output to input voltage for the P3219-A Coilcraft choke in which the turns ratio of the transformer is changed from 0.5 to 0.06. (a) 10 Hz–6 MHz linear frequency range (b) 10 Hz–30 MHz frequency range. Signal 1 is the response of the inductor without cancellation. Signal 2 is the performance with cancellation using a turns ratio $m=0.5$ and $C_p=56$ pF. Signal 3 is the response with cancellation using a turns ratio $m=0.06$ and $C_p=59$ pF. Note that the frequency scale is linear in both cases.

a turns ratio of 0.5. However, this capacitance, when considered with the leakage inductance in the compensation branch, leads to the system with the best performance at the frequencies of interest. Assuming that the transformer with 10.8-mH primary inductance has a coupling coefficient is 0.98 in both cases, the value of $C_{Comp} L_{Comp}$ changes from $3.024 \cdot 10^{-15}$ H F to $3.81 \cdot 10^{-17}$ H F when the turns ratio changes from 0.5 to .06. A comparison of the performance of the two cases of capacitance cancellation is shown in Fig. 5. Fig. 5(a) shows that the system with the lower turns ratio outperforms the other system at frequencies below 6 MHz, and using a lower turns ratio will raise the self-resonant frequency from 400 kHz to 1.4 MHz. The compensation capacitors were chosen in both cases to improve performance below 6 MHz. Signal 1 is the result of the normal inductor and signal 2 is the result of the inductor with capacitance cancellation with a turns ratio of 0.5 and a compensation capacitor of 56 pF. The system is changed such that the turns ratio is 0.06 and the compensation capacitor is 59 pF and the performance is improved to signal 3. Fig. 5(b) shows that above 6 MHz the performance of all three systems are dominated by other parasitics and that each system will outperform the others over some frequency range.

The model of the inductor used in Fig. 5 cannot be accurately described using Fig. 1 for the frequency range of interest. All three positive sloped regions in Fig. 5 (300 kHz–5 MHz, 6 MHz–8.5 MHz, and 10 MHz–22 MHz) represent areas in which the inductor looks capacitive, each region with a different capacitance. (A more accurate model of the inductor includes an two LC branches in parallel with the existing model of Fig. 1.) Capacitance cancellation can target any one of these three capacitances—with different values of the compensation capacitor—but over the other regions the capacitance cancellation winding will either not be optimal, or in the case of Fig. 5, harmful for the operation of the filter. Thus, depending on the frequency range of interest the compensation capacitor can be chosen to provide improved filtration.

In order to quantitatively evaluate the effects of the coupling coefficient on performance, a PSpice model of the experimental system leading to Fig. 4 was created (without the higher order parasitics). The parasitic capacitance of the inductor was set to 15 pF and the coupling coefficient was varied between 0.98 and 1. The simulated filter attenuation at 20 MHz is plotted as a function of the coupling coefficient in Fig. 6. This figure shows that the effectiveness of capacitance cancellation is very sensitive to

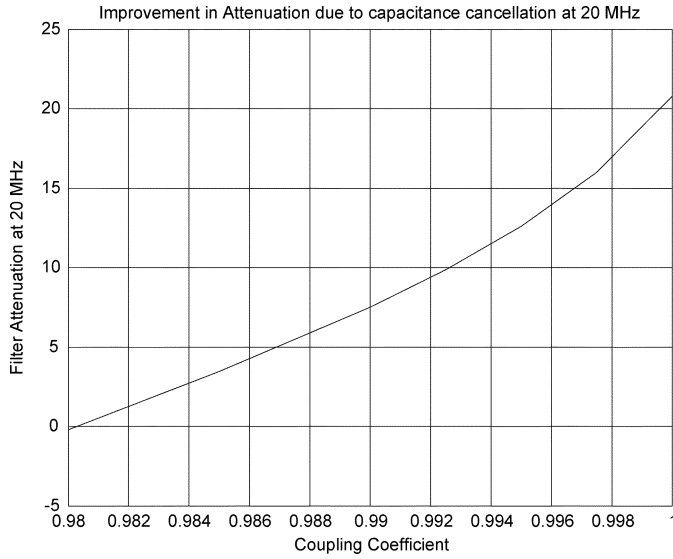


Fig. 6. Effects of changing the coupling coefficient on the system in Fig. 4. The parasitic capacitance of the inductor is 15 pF, the magnetizing inductance is 50 μ H, and the turns ratio (m) is 0.5.

the coupling coefficient. This insight is also relevant to other passive EMI cancellation techniques, such as those in [5]–[8].

This test was expanded to take into consideration changes in the turns ratio and changes in the amount of inductance and capacitance of the inductor under test. Fig. 7 shows a normalized plot of the filter attenuation at 20 MHz as a function of the term $C_{Comp}L_{Comp}$. Each point on the plot shows a set of simulations with different leakage inductances with a unique turns ratio, magnetizing inductance, and parasitic capacitance. Since some of the systems have different parasitic capacitances the total amount of possible attenuation improvement will be different. Thus, for each set of simulations the amount of attenuation is given as a percentage of the maximum possible case (15 to 30 dB depending on the case). The three outlying cases marked with diamonds represent cases in which the turns ratio is 0.125, otherwise a clear relationship exists between the relative improvement in attenuation and the term $C_{Comp}L_{Comp}$. Further analysis of the data used to generate this plot shows other trends, in particular that as the turns ratio, m , decreases, the range of the transformer's coupling coefficients over which beneficial results occur will increase. In other words, transformers with high coupling coefficients, for example, 0.9975 can be used with high turns ratios (0.75) to achieve good results, but a transformer with a lower coupling coefficient of 0.985 will need a system with a lower turns ratio (0.375) in order to get a similar improvement. The higher points in the figure correspond to systems with either low turns ratios or high coupling coefficients (or both), thus a transformer with near ideal coupling will lead to the overall best system possible.

IV. ALTERNATIVE IMPLEMENTATION

Here, we introduce an alternative implementation of the capacitance cancellation technique that avoids the magnetic coupling limitations of the simple implementation. Rather than relying on the limited magnetic coupling achievable with an additional winding on the filter inductor, the alternative implementation achieves the cancellation using a separate radio-frequency

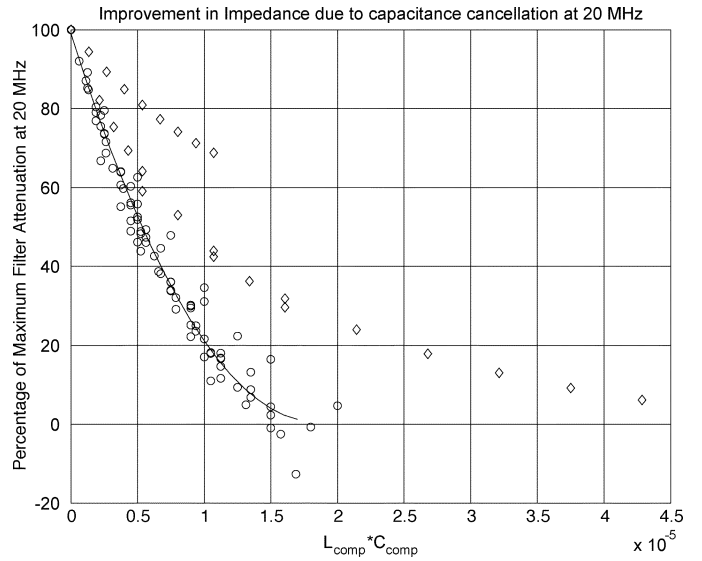


Fig. 7. The term $C_{Comp}L_{Comp}$, which is the total series capacitance and inductance in the compensation path, affects the amount of improvement this technique achieves. Every point in this plot corresponds to a simulation with a different magnetizing inductance, parasitic capacitance and turns ratio of the transformer. Two sets of data, corresponding to simulations with low turns ratios (marked with diamonds) and medium to high turn ratios (marked with circles) are shown. The data shows a definite trend, as illustrated by a best-fit curve to the second data set.

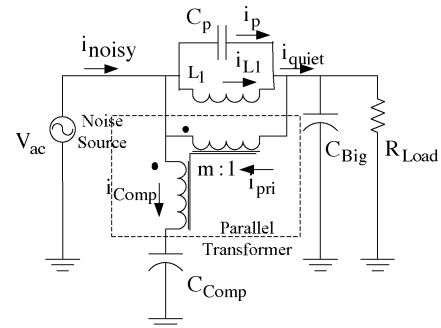


Fig. 8. Equivalent circuit model showing how capacitance cancellation can be implemented using a parallel RF transformer to inject cancellation currents.

(RF) transformer in parallel with the filter inductor, as illustrated in Fig. 8. The compensation capacitor is selected to compensate the parasitic capacitances of both the transformer and inductor. As will be shown, this technique can achieve highly effective capacitance cancellation using only small, inexpensive components.

The tradeoffs that arise in designing the inductor/transformer combination are similar to those that occur in some types of active EMI filters [22]. These design tradeoffs are summarized here. First, the RF transformer should have a high coupling coefficient to enable good capacitance cancellation to be achieved. The transformer magnetizing inductance should be similar to or larger than the original filter inductance to realize the desired filtering performance because it is desirable to have the majority of the current going through the original filter. Since it only needs to carry the small cancellation currents, the RF transformer can be wound with very fine wire, and can be made quite small and inexpensive. Differences in winding resistances between the RF transformer and filter inductor can be used to ensure that low-frequency currents flow through the filter inductor,

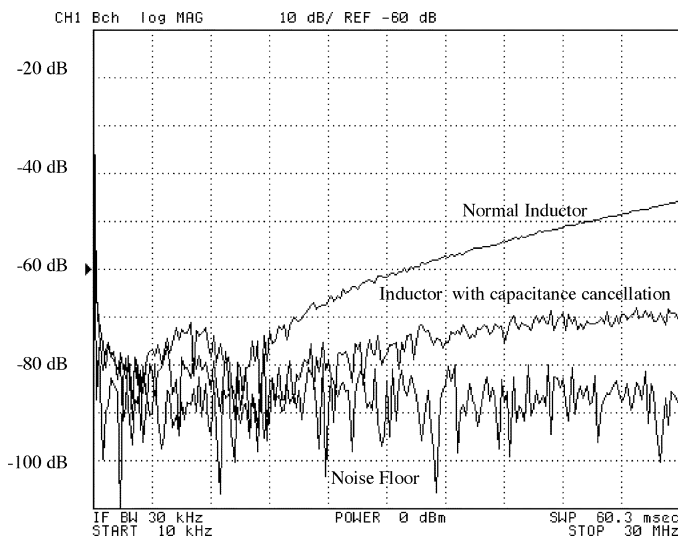


Fig. 9. Performance of a filter inductor with and without capacitance cancellation. The inductor (L_1 as shown in Fig. 8) is a packed RM12 core with 1 mH of inductance and the cancellation transformer is a Coilcraft WB3010.

though a small blocking capacitor could also be introduced for this purpose. One RF transformer meeting these criteria is the WB3010-1 (Coilcraft, Cary, IL). This center-tapped transformer has a magnetizing inductance of 760 μH and a coupling coefficient exceeding 0.999 in a six-pin DIP package. Because the transformer is center-tapped, a 2:1 transformer is easily be created (i.e., by connecting the full winding of the primary and only half the winding on the secondary) making this design suitable for capacitance cancellation applications.

The system shown in Fig. 8 was tested in the test setup of Fig. 2. The filter inductor is one half of a 1-mH common-mode choke constructed with 12 turns fully packed on an ungapped RM12 core. The 1-mH inductor, developed for automotive filtering applications, has approximately 20 pF of parasitic capacitance. The quiet-port bypass capacitance comprises the parallel combination of a 10- μF tantalum capacitor and a 1- μF ceramic capacitor. The transformer in parallel with the inductor is the WB3010, and an 86-pF ceramic capacitor is used. Experimental results for this prototype system are shown in Fig. 9. The highest curve shows the performance without the compensation circuit. The middle trace shows the performance with the capacitance cancellation. The lowest curve shows the noise floor of the network analyzer (the measured response with the test circuit disconnected). Capacitive cancellation improves the attenuation by 25 dB at 30 MHz.

To use this approach one must determine whether a small transformer can be placed in parallel with a large inductor by examining all the impedances of interest. In the case of the example above the inductor is a 1 mH inductance with 8 m Ω of resistance and the transformer used has a magnetizing inductance of 780 μH and a resistance of 320 m Ω . The impedance of the inductor ($R_i + jL_i\omega$) and the impedance of one set of windings of the transformer ($R_t + jL_t\omega$) form a current divider that sets a ratio of current distribution. This ratio will be dominated by either the resistances or inductances at low and high frequencies. At dc the transformer will see 40 times less current than the inductor. The impedance of the inductor will dominate the net parallel impedance up to 135 Hz, at which point the impedance

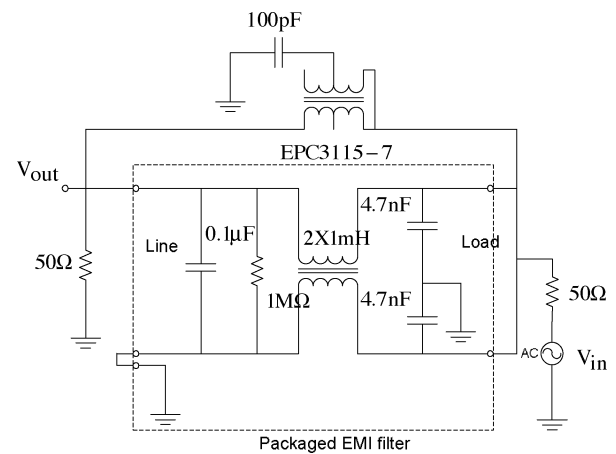


Fig. 10. Schematic for the common mode choke with capacitance cancellation and setup for a common mode test. The two added elements, the EPC3115-7 transformer and the 100-pF capacitor, are located on the case of the filter. A common mode signal is introduced from the load side of the filter and the common mode noise is measured on the line side of the filter.

of the transformer will dominate. In order to alter the balance the ratio of dc currents even further, added elements, such as capacitors or resistors can be placed in series with the transformer. This can be used to further decrease the amount of dc current that the transformer has to pass and make the technique applicable to high current applications. Thus, the goal of this circuit approach is for the inductor to be the lowest impedance path at dc and low frequencies which contain significant ripple currents such that the transformer can be made small. Note, that the magnetizing inductance of the transformer should be kept significantly larger than the original inductance, unless some degree of performance degradation at low frequency is tolerable. Also, note that any capacitance introduced by the transformer can be cancelled along with the capacitance of the original inductor.

Capacitance cancellation was also applied to improve the common mode performance of an EMI filter. A commercial EMI line filter, the Schaffner FN2010-6-06, is used to test capacitance cancellation. The filter is a one stage filter and is shown in Fig. 10. The parasitic capacitance, as measured across either the positive or negative terminals, is 31 pF. A small center-tapped transformer, EPC3115-7 from PCA Electronics Inc., is added outside the filter case. This transformer has a turns ratio of 1:1.5, so the secondary is connected across the filter and the primary is used for the compensation path. A picture of the modified circuit is shown in Fig. 11. A variety of compensation capacitors were experimentally tested and a ceramic 100-pF capacitor was chosen. This capacitor is connected from the center-tap of the transformer primary to the ground (i.e., the enclosure). The modified circuit and the common mode test setup are shown in Fig. 10.

The resulting circuit has better performance at high frequencies. The parasitic capacitance of the filter choke is the dominant limit to attenuation at frequencies over 1 MHz until the self-resonance of the Y-capacitors (The capacitors from either line to ground) at 23 MHz. In this range of frequencies, the filter with parasitic capacitance cancellation has better performance. An improvement of at least 10 dB in attenuation is achieved from 3 to 20 MHz and an improvement of 20 dB is achieved at 14 MHz. Results of this test are shown in Fig. 10.

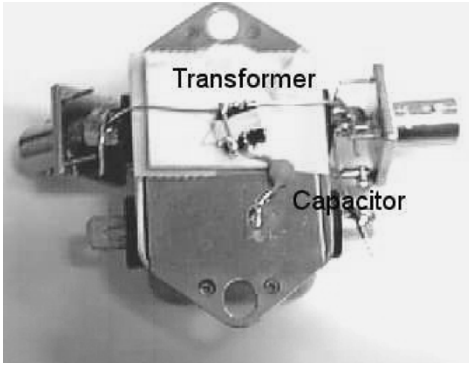


Fig. 11. Photograph of the FN2010-6-06 filter with external capacitance cancellation. Only a small transformer and ceramic capacitor are needed to improve performance.

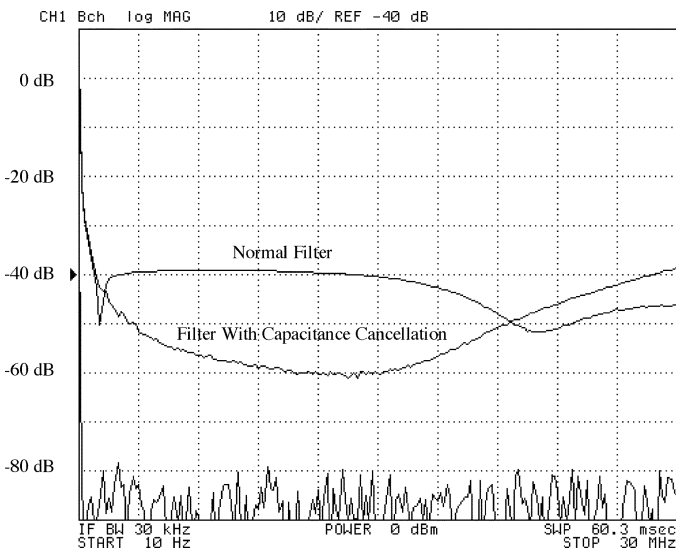


Fig. 12. Plot comparing the performance of the common mode response of an EMI filter, Schaffner FN2010-6-06, and one modified with capacitance cancellation as shown schematically in Fig. 8. Note that the frequency range is linear and up to 30 Mhz.

With the configuration of Fig. 12 a common mode input signal will cause a differential mode signal across the load due to the unbalanced manner in which the capacitor is cancelled. An ideal PSpice simulation of the system indicates up to a 64-mV differential signal may occur on the output due to a 1-V common mode disturbance, as shown in Fig. 13. The unmodified filter is balanced, and no common-mode to differential-mode transfer exists. The filter with capacitance cancellation on only one side of the choke thus has the possibility of worsening differential-mode performance. However, if this is a concern, capacitance cancellation can be applied in a balanced fashion (i.e., on both sides of the choke) thereby eliminating any such transfer.

The use of capacitance cancellation does have some side effects. As mentioned previously, the current from the noisy port will increase due to capacitance cancellation. Although the parasitic capacitance can be cancelled, ideal performance at all frequencies is not practical. Ideally an inductor with no parasitic capacitance will have an impedance proportional to frequency. Thus, ideally, assuming a capacitor with no parasitic inductance, an L -section filter will have a 40-dB roll off from

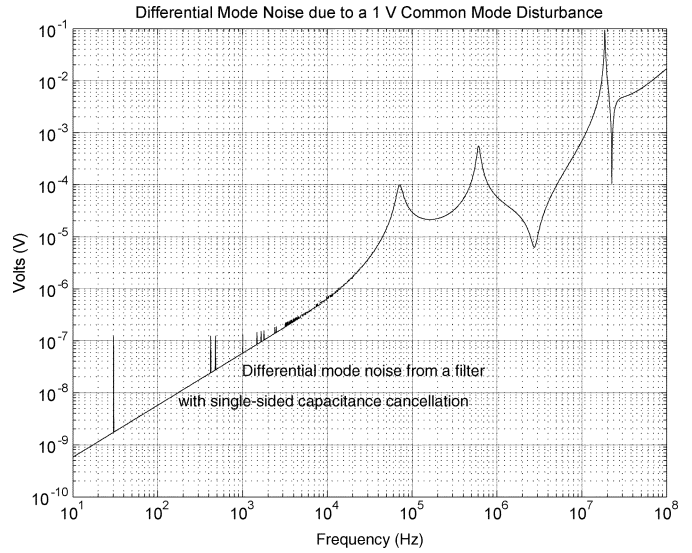


Fig. 13. PSpice simulation examining the differential mode noise that results from a common mode disturbance for the system shown in Fig. 8. The common-mode to differential-mode noise transfer performance of the unmodified filter is essentially zero.

the resonant frequency onward. Real performance is not this good, mainly due to the impedance of the compensation branch. The compensation branch impedance consists of the real capacitor, leakage inductance, and parasitic resistance in series. Assuming that all the other parasitic elements are negligible then the voltage $v_{ac}(1 - m)$ appears across the compensation branch. The current induced in the secondary of the transformer (and therefore proportional to the current in the primary) will be controlled in order to divert the current “traveling” in the parasitic capacitor away from the quiet port. At low frequencies the compensation impedance is dominated by the capacitance and thus the current in the primary winding of the transformer is $v_{ac}(1 - m)mC_{comp}j\omega$ which is equal to the current due to the parasitic capacitance (i.e., $v_{ac}C_p$) assuming the proper turns ratio and compensation capacitor.

At higher frequencies the impedance of the leakage inductance of the transformer will dominate the compensation impedance. When the compensation impedance is inductive then the current in the primary winding of the transformer is $v_{ac}(1 - m)m(1/L_sj\omega)$. This current will not decrease, but rather increase the amount of unwanted current going into the quiet port. Fortunately as frequency increases this current will decrease but as seen in Fig. 12 there will be a frequency range in which the normal inductor outperforms the inductor with capacitance cancellation. Other than the secondary leakage inductance, capacitance cancellation will have parasitic components (such as primary leakage inductance and capacitance from the primary to secondary winding of the transformer) that will also affect high frequency performance.

V. CONCLUSION

This paper introduces a technique for improving the high-frequency performance of filter inductors and common-mode chokes by cancelling out the effects of parasitic capacitance. This technique uses additional passive components to inject a compensation current that cancels the current flowing through

the inductor parasitic capacitance, thereby improving high-frequency filtering performance. The main problem with realizing capacitance cancellation is creating a compensation impedance that exactly corresponds to the parasitic capacitance. Any extra inductance in this path, which can easily be created by the leakage inductance of the transformer, will impair performance. More specifically, the performance of the system is related to the ratio of inductive reactance to capacitive reactance in the compensation branch. Two implementation approaches for this technique are introduced. The first implementation achieves cancellation using an additional small winding on the filter inductor and a small capacitor. This approach is effective where either very high coupling of the windings can be achieved or the turns ratio is very low. The second implementation uses a small RF transformer in parallel with the filter inductor to inject cancellation currents from the compensation capacitor. This technique requires an additional component (the transformer), but can provide a high degree of cancellation. Experimental results confirm the theory in both implementations. The application of this technique to a commercial EMI filter has been shown to improve common-mode attenuation by up to 20 dB.

The main differences between these two techniques lie in the nature of the inductor in which capacitance is to be cancelled. If the inductor can be changed into a high quality transformer with a high coupling coefficient, than the first method is advantageous. An additional component can be used in case the target inductor makes a poor transformer; the tradeoff then becomes a question of cost between inductors and transformers. The choice between the two different methods will also affect the design effort. Typically it is easier to purchase or develop an additional high frequency transformer than it is to rewind an inductor that works well at high frequency into an effective transformer using different wire gauges and without a 1:1 winding ratio.

REFERENCES

- [1] H. Ott, *Noise Reduction Techniques in Electronic Systems*, 2nd ed. New York: Wiley, 1988, ch. 5.
- [2] A. Massarini, M. Kazimierczuk, and G. Grandi, "Lumped parameter models for single- and multiple-layer inductors," in *Proc. IEEE PESC Conf.*, Jun. 1996, pp. 295–301.
- [3] A. Massarini and M. Kazimierczuk, "Self-capacitance of inductors," *IEEE Trans. Power Electron.*, vol. 12, no. 4, pp. 671–676, Jul. 1997.
- [4] M. Kazimierczuk, G. Sancineto, G. Grandi, U. Reggiani, and A. Massarini, "High-frequency small-signal model of ferrite core inductors," *IEEE Trans. Magnetics*, vol. 35, no. 5, pp. 4185–4191, Sep. 1999.
- [5] W. Xin, F. Poon, C. Lee, M. Pong, and Z. Qian, "A study of common mode noise in switching power supply from a current balancing viewpoint," in *Proc. IEEE Int. Conf. Power Electronics Drive Systems*, 1999, pp. 621–625.
- [6] W. Xin, M. Pong, Z. Lu, and Z. Qian, "Novel boost PFC with low common mode EMI: modeling and design," in *Proc. IEEE Applied Power Electronics Conf.*, 2000, pp. 178–181.
- [7] M. Kchikach, Z. Qian, X. Wu, and M. Pong, "The influences of parasitic capacitances on the effectiveness of anti-phase technique for common mode noise suppression," in *Proc. IEEE Int. Conf. Power Electronics Drive Systems*, vol. 1, Oct. 2001, pp. 115–120.
- [8] D. Cochrane, D. Chen, and D. Boroyevic, "Passive cancellation of common-mode noise in power electronic circuits," *IEEE Trans. Power Electron.*, vol. 18, no. 3, pp. 756–763, May 2003.
- [9] M. Shoyama, T. Okunaga, G. Li, and T. Ninomiya, "Balanced switching converter to reduce common-mode noise," in *Proc. IEEE Power Electronics Specialists Conf.*, Jun. 2001, pp. 451–456.

- [10] M. Shoyama, M. Ohba, and T. Ninomiya, "Balanced buck-boost switching converter to reduce common-mode conducted noise," in *Proc. IEEE PESC*, Jun. 2002, pp. 2056–2061.
- [11] G. Crouse, "Electrical filter," U.S. Patent 1 920 948, Aug. 1, 1933.
- [12] S. Feng, W. Sander, and T. Wilson, "Small-capacitance nondissipative ripple filters for dc supplies," *IEEE Trans. Magnetics*, vol. 6, no. 1, pp. 137–142, Mar. 1940.
- [13] G. Bloom and R. Severns, "The generalized use of integrated magnetics and zero-ripple techniques in switchmode power converters," in *Proc. IEEE PESC*, Jun. 1984, pp. 15–33.
- [14] R. Severns and G. Bloom, *Modern DC-to-DC Switchmode Power Converter Circuits*. New York: Van Nostrand Reinhold, 1985.
- [15] J. Kolar, H. Sree, N. Mohan, and F. Zach, "Novel aspects of an application of 'zero'-ripple techniques to basic converter topologies," in *Proc. IEEE PESC*, Jun. 1997, pp. 796–803.
- [16] S. Senini and P. Wolfs, "The coupled inductor filter: analysis and design for AC systems," *IEEE Trans. Ind. Electron.*, vol. 45, no. 4, pp. 574–578, Aug. 1998.
- [17] D. Hamill and P. Krein, "A 'zero' ripple technique applicable to any dc converter," in *Proc. IEEE PESC*, Jun. 1999, pp. 1165–1171.
- [18] T. Neugebauer, J. Phinney, and D. Perreault, "Fillers and components with inductance cancellation," *IEEE Trans. Ind. Appl.*, vol. 40, no. 2, pp. 939–947, Mar. 2004.
- [19] T. Neugebauer and D. Perreault, "Filters and inductance cancellation using printed circuit board transformers," *IEEE Trans. Power Electron.*, vol. 19, no. 3, pp. 272–282, May 2004.
- [20] F. Terman, *Electronic and Radio Engineering*, 4th ed. New York: McGraw-Hill, 1955.
- [21] T. Lee, *The Design of CMOS Radio-Frequency Integrated Circuits*. New York: Cambridge Univ. Press, 1998, ch. 1, pp. 16–17.
- [22] A. Chow and D. Perreault, "Design and evaluation of a hybrid passive/active ripple filter with voltage injection," *IEEE Trans. Aerosp. Electron. Syst.*, vol. 39, no. 2, pp. 471–480, Apr. 2003.



Timothy C. Neugebauer received the B.S. degree in electrical engineering from Union College, Schenectady, NY, in 1997 and the M.S. and Ph. D. degrees from the Massachusetts Institute of Technology, Cambridge, in 1999 and 2004, respectively.

He currently works for Draper Laboratories, Cambridge, MA.



David J. Perreault (M'98) received the B.S. degree from Boston University, Boston, MA, in 1989, and the S.M. and Ph.D. degrees from the Massachusetts Institute of Technology (MIT), Cambridge, in 1991 and 1997, respectively.

In 1997, he joined the MIT Laboratory for Electromagnetic and Electronic Systems as a Postdoctoral Associate, and became a Research Scientist in the laboratory in 1999. In July 2001, he joined the MIT Department of Electrical Engineering and Computer Science, where he is presently the Emanuel

E. Landsman Associate Professor of Electrical Engineering and Computer Science. His research interests include design, manufacturing, and control techniques for power electronic systems and components, and in their use in a wide range of applications.

Dr. Perreault received the Richard M. Bass Outstanding Young Power Electronics Engineer Award from the IEEE Power Electronics Society and an ONR Young Investigator Award. He is a member of Tau Beta Pi and Sigma Xi.